Global Dynamics of Mechanical Systems with Cubic Potentials

M. Falconi

*Depto. de Matemáticas, Fac. de Ciencias, UNAM.C. Universitaria, México, D.F.
04510*
E-mail: falconi@servidor.unam.mx

and

E.A. Lacomba

Mathematics Department,UAM-I. P.O.Box 55-534, México, D.F. 09340
E-mail: lace@xanum.unam.mx

and

C. Vidal

*Departamento de Matematicas, Universidade Federal de Pernambuco,Cidade
Universitaria. Recife-Pe, Brasil*
E-mail: claudio@riemann.dmat.ufpe.br

Submitted by J. Llibre

We study the behavior of solutions of mechanical systems with polynomial
potentials of degree 3 by using a blow up of McGehee type. We first state some
general properties for positive degree homogeneous potentials. In particular,
we prove a very general property of transversality of the invariant manifolds of
the flow along the homothetic orbit . The paper focuses in the study of global
flow in the case of homogeneous polynomial potentials of degree 3 for negative
energy. The flow is fairly simple because of its gradient-like structure, although
for some values of the polynomial coefficients we have diverse behaviour of the
separatrices on the infinity manifold, which are essential to describe the global
flow.

Key Words: Hamiltonian Vector Field, Homogeneous Polynomial Potentials,
Invariant Manifolds, Global Flow

1. INTRODUCTION

In a previous paper [5] we studied the asymptotic behavior of the solutions escaping to the infinity of configuration space for mechanical systems with polynomial potentials of degree at most 4. The essential tool is the application of a McGehee type blow up at infinity studied systematically by Lacomba and Ibort [8]. McGehee [10] introduced his blow up transformation for the study of the neighborhood of triple collision in the rectilinear three body problem. It was then extended in a more or less straightforward way to the study of the total collapse in any n-body problem in Celestial Mechanics.

Since we consider mechanical systems with two degrees of freedom, the blow up at infinity glues as a boundary to any energy level a compact surface, which is invariant under the extended flow. Since the equilibrium points are generically hyperbolic, understanding of the flow in this compact surface gives asymptotic information on solutions escaping to infinity.

In Section 2 we begin by recalling some general properties of the blow up at infinity and the flow on the energy levels and the infinity surface for mechanical systems with 2 degrees of freedom and any positive degree of homogeneity. It turns out that the flow on the infinity surface is always gradient-like with respect to one of the velocity coordinates. These results were proved in [5]. Then we prove the transversality of some invariant manifolds of the flow.

In Section 3 we restate the main properties of the flow and the topology of the infinity manifold for cubic homogeneous potentials, which were proved in [5] and turned out to be fundamental for studying the global flow. We include now a new symmetry property of the flow for potentials of the form $y^3 + \beta x^3$.

In Section 4 we analyze the global flow on negative energy levels for the case when the flow on the infinity manifold has 2 saddle points. The other cases are trivial due to the gradient-like structure of the flow. Finally, in Section 5 we include some numerical simulations to visualize the behavior of the flow described in the previous section. For completeness, other simulations are considered for giving a sketch of the flow for positive energy.

The study of this class of mechanical systems with polynomial potentials of degree 3 is based on the normal form which is described in Section 3. A typical example of this situation is the Hamiltonian in $\mathbb{R}^2$ with Henon-Heiles polynomial potential

$$V\left(x,y\right) = -\alpha\left(x\,y^2 - x^3/3\right),$$

considered in [8]. Its normal form is

$$U\left(X,Y\right) = Y^3 - 3X^2Y.$$

This class of potentials was considered by Grammaticos and Dorizzi [6] , in order to classify the integrable cases.

2. GENERAL PROPERTIES FOR POSITIVE DEGREE.

In this section we study some general properties for mechanical systems with homogeneous potentials of positive degree. Our two degrees of freedom Hamiltonian system has then the form

$$H\left(x, y, p_1, p_2\right) = \frac{1}{2}\left(p_1^2 + p_2^2\right) - V\left(x, y\right) \tag{1}$$

where V is a homogeneous function of degree $d > 0$ in the plane, i.e. $V\left(\lambda x, \lambda y\right) = \lambda^d V\left(x, y\right)$ for any $\lambda > 0$.

In order to apply a blow up at infinity, configuration coordinates are changed into polar coordinates, but with the radial coordinate replaced by its reciprocal. The new position coordinates are ρ, θ, where

$$\rho = \frac{1}{\sqrt{x^2 + y^2}}; \ x = \frac{1}{\rho}\cos\theta; \ y = \frac{1}{\rho}\sin\theta. \tag{2}$$

Since the energy relation has to be regular at $\rho = 0$, the new radial and tangential velocity components are respectively defined as

$$v = \rho^{d/2}\left(-\dot{\rho}/\rho^2\right), \ u = \rho^{d/2}\left(\rho^{-1}\dot{\theta}\right). \tag{3}$$

Then the energy relation $H = h$ in ρ, θ, v, u coordinates becomes

$$\frac{1}{2}\left(u^2 + v^2\right) = U\left(\theta\right) + \rho^d h, \tag{4}$$

where $U\left(\theta\right) = V\left(\cos\theta, \sin\theta\right).$

Writing Hamilton's equations for Hamiltonian (1) in terms of the new variables, shows the further need for a change of time scale

$$\frac{dt}{d\tau} = \rho^{d/2-1}, \tag{5}$$

in order to eliminate this factor from the right hand side of all the equations. We obtain the following system of differential equations

$$\begin{array}{ll} \rho' = -\rho\ v, & v' = u^2 - \frac{d}{2}\ v^2 + d\ U\left(\theta\right), \\ \theta' = u, & u' = -\frac{d+2}{2}u\ v + U'\left(\theta\right), \end{array} \tag{6}$$

where $' = d/d\tau$.

The energy level $H = h$ in the new coordinates is defined as the 3-dimensional manifold

$$E_h = \left\{ (\rho, \theta, v, u) \mid \rho > 0, \ \frac{1}{2} \left(u^2 + v^2 \right) = U(\theta) + \rho^d h \right\}.$$

But since the energy relation (4) and the system of equations (6) are well defined at infinity, i.e. $\rho = 0$, we can glue to E_h a 2-dimensional boundary, the so-called *infinity surface*

$$N_\infty = \left\{ (\rho, \theta, v, u) \mid \rho = 0, \ \frac{1}{2} \left(u^2 + v^2 \right) = U(\theta) \right\},$$

which is independent of h and invariant under the flow, because from (6) $\rho = 0$ implies $\rho' = 0$. Although E_h and N_∞ are contained in a 4-dimensional space, they can be represented in the 3-space of coordinates θ, v, u when $h < 0$ or $h > 0$. The boundary N_∞ is a surface of revolution defined only at points where $U \geq 0$.

For $h \neq 0$ the equilibrium points are defined by the conditions

$$\rho = 0, \ U'(\theta) = 0, \ v = \pm\sqrt{2U(\theta)}, \ u = 0.$$

This means that we have 2 equilibria for each critical point θ of U where $U(\theta) > 0$, but only one degenerate equilibrium if $U(\theta) = 0$. It is easy to prove the following result

PROPOSITION 1. *If $U(\theta_0) > 0$, $U'(\theta_0) = 0$ and $U''(\theta_0) \neq 0$, the corresponding equilibrium points are hyperbolic for the flow.*

Under the conditions of the above proposition, we see that

a) If $U_0'' < 0$, the equilibrium point is an attractor if $v_0 > 0$ and repeller if $v_0 < 0$. There is a spiralling if $k^2 v_0^2 + 4U_0'' < 0$.

b) If $U_0'' > 0$, the equilibrium points are saddles.

If $U''(\theta_0) > 0$, the non degenerate equilibrium point S_+ with $v(\theta_0) = \sqrt{2U(\theta_0)}$ has a 2-dimensional stable manifold $W^s(S_+)$ and the equilibrium point S_- with $v(\theta_0) = -\sqrt{2U(\theta_0)}$ has a 2-dimensional unstable manifold $W^u(S_-)$.

The critical points of U generate the so-called *homothetic solutions*. These are the simplest possible solutions of (6), defined by taking $\theta \equiv \theta_0$ where $U'(\theta_0) = 0$. That implies $u = \theta' = 0$, which agrees with $u = 0$. We are left with only 2 equations

$$\begin{aligned}
\rho' &= -\rho\, v, \\
v' &= d\left(-\tfrac{v^2}{2} + U(\theta_0) \right),
\end{aligned} \tag{7}$$

which can be explicitly integrated to get $\rho(\tau)$ and $v(\tau)$. Homothetic solutions are depicted as vertical lines for $h \neq 0$ in θ, v, u coordinates. When $U''(\theta_0) > 0$, the homothetic solution belongs to the intersection of the manifolds W^s and W^u.

A flow is *gradient-like* with respect to a function g, if g is strictly increasing along solution curves of the flow, unless the solution is an equilibrium point. In [5] the following proposition was proved.

PROPOSITION 2. *The flow of (6) is gradient-like with respect to v, as follows*

(a)*If $h < 0$ on $E_h \cup N_\infty$ $(\rho \geq 0)$*
(b)*If $h \geq 0$ on N_∞ $(\rho = 0)$*

To analyze the geometrical structure of the manifolds W^s and W^u along the homothetic orbit it is useful to point out the symmetry

$$(\rho, \theta, v, u, \tau) \rightarrow (\rho, \theta, -v, -u, -\tau) \tag{8}$$

of the system (6).

This symmetry implies that the orbit $(\rho(\tau), \theta(\tau), v(\tau), u(\tau))$ converges to S_+ when τ tends to ∞, if and only if $(\rho(-\tau), \theta(-\tau), -v(-\tau), -u(-\tau))$ converges to S_- when τ tends to $-\infty$.

The variational equations along the homothetic orbit are given by

$$\begin{aligned} \theta' &= u, \\ v' &= -dv(t)v, \\ u' &= U_0''\theta - \left(\tfrac{d+2}{2}\right)v(\tau)u, \end{aligned} \tag{9}$$

where $U_0'' = U''(\theta_0)$.

We parametrize the homothetic orbit ξ in such a way that $\xi(0)$ belongs to the plane $\{v = 0\}$. Let us consider a small neighbourghood around $\xi(0)$. Let β_0^- be the curve which is obtained from intersecting W^u with $\{v = 0\}$ within that neighbourghood. We denote by $T\beta_0^-$ the tangent vector to β_0^- at the point $\xi(0)$ and by φ_τ the flow of the vector field (6). When the curve β_0^- is transported by the flow φ_τ, we get the curve $\varphi_\tau\left(\beta_0^-\right)$, whose tangent vector at $\xi(\tau)$ is given by $T\beta_\tau^- = D\varphi_\tau(\xi(\tau)) \cdot T\beta_0^-$. This vector is tangent to the manifold W^u at the point $\xi(\tau)$, and it follows from Equation (9) that its component in the direction v is zero.

When τ tends to $-\infty$, we have that $\xi(\tau) \rightarrow S_-$, then by continuity of the vector field (6) it follows that $T\beta_\tau^-$ converges to a vector $T\beta_{-\infty}^-$, which is tangent to the manifold W^u at the point S_-. Since $T\beta_\tau^-$ has a null component along the direction v, the same happens with $T\beta_{-\infty}^-$, then this

vector is also tangent to N_∞. Analogously a vector $T\beta_\infty^+$ is constructed for the manifold W^s.

Let $\alpha^\pm(\tau)$ be the argument of the projection onto the plane $\{(\theta, u)\}$ of the vector $T\beta_\tau^\pm$. From the symmetry (8) the equality $\alpha^+(\tau) = -\alpha^-(-\tau)$ follows. So, if the manifolds W^s and W^u do not intersect transversally along the homothetic orbit, then the increment of α^-, from $T\beta_0^-$ until $T\beta_{-\infty}^-$ must to be at least $\pi/2$. In this way we have proved the following result

LEMMA 3. *Suppose that $U''(\theta_0) > 0$ and $h < 0$. The manifolds W^s and W^u intersect transversally along the homothetic orbit if the increment of $\alpha^\pm(\tau)$ from $T\beta_0^\pm$ to $T\beta_{\pm\infty}^\pm$ is smaller than $\pi/2$.*

We prove in the following theorem, the transversaliy of W^s and W^u along the homothetic orbit.

THEOREM 4. *Let $U(x, y)$ be a homogeneous polynomial potential of degree $d > 0$. Suppose that $h < 0$, $U(\theta_0) > 0$, $U'(\theta_0) = 0$ and $U''(\theta_0) > 0$. Then the stable manifold $W^s(S_+)$ and the unstable manifold $W^u(S_-)$ intersect transversally along the homothetic trajectory $\{\theta = \theta_0, u = 0\}$.*

Proof. Let (R, α) be polar coordinates in the plane $\{\theta, u\}$. So, we have

$$\theta = R\cos\alpha, \ u = R\sin\alpha. \tag{10}$$

Thus, we get

$$\alpha' = \frac{d}{d\tau}\left(\arctan\frac{u}{\theta}\right) = \frac{1}{u^2 + \theta^2}(\theta u' - u\theta').$$

Using now the variational equation, we obtain the equation

$$\alpha = \frac{1}{R^2}\left(U_0''\theta^2 - \left(\frac{d+2}{2}\right)\theta vu - u^2\right). \tag{11}$$

The solution of Equation (7) with initial condition $v(0) = 0$ is given by

$$v(\tau) = \sqrt{2U_0}\tanh\left(\frac{d}{2}\sqrt{2U_0}\tau\right). \tag{12}$$

In view of the relations (10), (12) for θ, u and $v(\tau)$, the equation (11) reduces to

$$\alpha' = a\cos^2\alpha - b\cos\alpha\sin\alpha\tanh(c\tau) - \sin^2\alpha = f(\alpha, \tau), \tag{13}$$

where $a = U_0''$, $b = \sqrt{2U_0}\left(\frac{d+2}{2}\right)$, $c = \frac{d}{2}\sqrt{2U_0}$.

We will prove now that the increment of α is smaller than $\pi/2$, which according to Lemma 3 implies the transversality of W^s and W^u.

To analyze (13) we consider the initial condition $\tau = 0$, $\alpha = \alpha_0$. Where α_0 is the unique solution of the equation $f(\alpha, 0) = 0$, on the interval $(0, \pi/2)$. For each $\tau > 0$, there exists a unique solution $\overline{\alpha}(\tau)$ of the equation $f(\overline{\alpha}(\tau), \tau) = 0$; equivalently, $\overline{\alpha}(\tau)$ satisfy

$$a \cos^2 \overline{\alpha}(\tau) - b \cos \overline{\alpha}(\tau) \sin \overline{\alpha}(\tau) \tanh(c\tau) = \sin^2 \overline{\alpha}(\tau). \qquad (14)$$

Since $\tanh(c\tau)$ is positive and increasing in $[0, \infty)$ and $b \cos \alpha \sin \alpha$ is positive in $(0, \pi/2)$, it follows from (14) that $\overline{\alpha}(\tau)$ is a decreasing function which is bounded below by 0. Moreover, as $\frac{\partial f}{\partial \alpha}(\overline{\alpha}(\tau), \tau) \neq 0$, $\overline{\alpha}(\tau)$ is differentiable. By a simple calculation we verify that the derivative $\overline{\alpha}'(0)$ is smaller than 0. This fact, together with $\alpha'(0) = 0$ and $\alpha(0) = \overline{\alpha}(0)$, imply that $\alpha(\tau) > \overline{\alpha}(\tau)$ for all τ in a small interval $(0, \tau_0)$. We will see that this inequality is satisfied for all $\tau > 0$. Indeed, if $\alpha(\tau_1) < \overline{\alpha}(\tau_1)$ for some $\tau_1 > 0$, then we take τ_0, the closest value of τ to τ_1 such that $\tau_0 < \tau_1$ and $\alpha(\tau_0) = \overline{\alpha}(\tau_0)$. Thus, $\alpha(\tau) < \overline{\alpha}(\tau)$ for all $\tau \in (\tau_0, \tau_1)$. However this is not possible, since $\overline{\alpha}'(\tau_0) < 0$ and due to the equality $f(\overline{\alpha}(\tau_0), \tau_0) = 0$, we have $\alpha'(\tau_0) = 0$.

Finally, notice that $f(\alpha, \tau) < 0$ for all $\alpha > \overline{\alpha}(\tau)$. Therefore $\alpha(\tau)$ is a decreasing function. The theorem follows from the inequality

$$\pi/2 > \alpha_0 > \alpha_0 - \overline{\alpha}(\tau) > \alpha_0 - \alpha(\tau) > 0.$$

∎

3. THE FLOW ON N_∞ FOR DEGREE 3

From now on we restrict ourselves to homogeneous polynomial potentials. By reducing to a normal form, we study the topology of the infinity surface and describe the flow on it. We consider just the case of degree 3.

The general form of a homogeneous polynomial potential of degree 3 with 2 degrees of freedom is

$$V(x, y) = ay^3 + bxy^2 + cx^2y + dx^3.$$

In order to study the different Hamiltonian flows up to diffeomorphism, let us consider a normal form of $V(x, y)$ up to canonical changes of coordinates with a constant rescaling of time, which also preserve the form of the kinetic energy. We obtain the normal forms

$$V(x, y) = \gamma y^3 + \alpha xy^2 + \beta x^3, \qquad (15)$$

$$V(x,y) = y^3 + \alpha xy^2 + \beta x^3, \text{if } \gamma \neq 0, \tag{16}$$
$$V(x,y) = \gamma y^3 + \alpha xy^2 + x^3, \text{ if } \beta \neq 0. \tag{17}$$

See details in [4]. Notice that (16) and (17) are particular cases of (15), while in the form (15) we still have to identify cubics differing by a nonzero scalar multiple. Let $[\gamma, \alpha, \beta]$ denote the class of nonzero scalar multiples of the vector $(\gamma, \alpha, \beta) \in \mathbb{R}^3 \setminus \{0\}$. The classes $[\gamma, \alpha, \beta]$ are homogeneous coordinates for the projective plane $\mathbb{R}P^2$. Hence, we can think of the cubic (15) as having coefficients in $\mathbb{R}P^2$. The normal form (16) corresponds to taking the plane $\{(1, \alpha, \beta) : \alpha, \beta \in \mathbb{R}\}$ in $\mathbb{R}^3$ as a chart for $\mathbb{R}P^2$. The normal form (17) corresponds to taking the plane $\{(\gamma, \alpha, 1) : \gamma, \alpha \in \mathbb{R}\}$ as another chart for $\mathbb{R}P^2$. Both charts provide a complete description of the projective plane.

We will analyze in detail potentials given by (16). Similar results are valid for (17), which is used in [6], after variables x and y are exchanged. Then we define the trigonometric polynomial $U(\theta)$ of degree 3

$$U(\theta) = V(\cos\theta, \sin\theta) = \sin^3\theta + \alpha\cos\theta\sin^2\theta + \beta\cos^3\theta,$$

whose derivative is given by

$$U'(\theta) = \sin\theta[-\alpha\sin^2\theta + (2\alpha - 3\beta)\cos^2\theta + 3\sin\theta\cos\theta].$$

As a consequence of Proposition 3.1 in [5], we can say that the homogeneous trigonometric polynomials U and U' of degree 3 can have $2k$ roots for $1 \leq k \leq 3$. Moreover, $U(\theta + \pi) = -U(\theta)$ and $U'(\theta + \pi) = -U'(\theta)$ for any θ. In particular if $U(\theta_0) = 0$, then $U(\theta_0 + \pi) = 0$ and the same is true for U'.

It is clear that the general shape and smoothness of the infinity surface N_∞ depend of the roots of $U(\theta)$ and of $U'(\theta)$.

DEFINITION 5. Given any homogeneous trigonometric polynomial $U(\theta)$, we say that U is of *type* $\{N_1, N_2\}$ if U has N_1 roots and U' has N_2 roots modulo 2π.

We see that N_1 and N_2 are always even numbers. From elementary Calculus we have $N_2 \geq N_1$. More precisely, for degree 3 we have

$$6 \geq N_2 \geq N_1 \geq 2. \tag{18}$$

There are only five different cases $\{2, 2\}$, $\{2, 4\}$, $\{2, 6\}$, $\{4, 6\}$ and $\{6, 6\}$, satisfying inequality (18). The function U and the topology of N_∞ in each case are depicted in Fig. 1. For type $\{2, 4\}$ we have 2 different shapes of N_∞, both of them having a degeneracy consisting of two inflection

points, which give rise to singular points of N_∞ in the case where they are located in the θ axis. In the other case, N_∞ is topologically as in $\{2, 6\}$, but the gradient-like flow on it suffers a bifurcation due to the inflection point with $U > 0$.
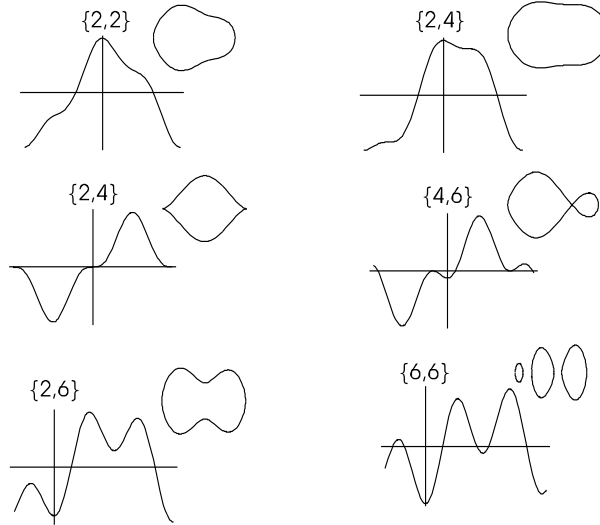
FIG. 1. Different shapes of the surface N_∞ in relation to the graph of the corresponding $U(\theta)$. The horizontal axes correspond to the variable θ.

We are concerned now with the description of the flow in E_∞ for negative energy. Because of the gradient-like structure, we need a flow description only for the open regions of the parameter values where the type is $\{2, 6\}$. At the points of the line $\beta = 2/3 \, \alpha$ the topology of N_∞ stays the same, but its flow bifurcates. The description of the flow in the above regions is not so simple, and we give only a partial description. We study thoroughly the case $\alpha = 0$ to begin with, so the potential takes the form,

$$V(x, y) = y^3 + \beta x^3. \tag{19}$$

The global flow for this case will be studied in Section 4.

For this potential, besides the symmetry (8), the system (6) has the symmetry $\beta \to 1/\beta$ when the potential is as in(19).

Let us consider the diffeomorphisms $F_1 : (x, y, p_1, p_2) \to (X, Y, P_1, P_2)$ and $F_2 : (r, \theta, v, u) \to (r, \phi, \mathfrak{v}, \mathfrak{u})$ given by,

$$X = y, \; Y = x, \; P_1 = \beta^{-1/2} p_2, \; P_2 = \beta^{-1/2} p_1, \tag{20}$$

and

$$\mathfrak{u} = -\beta^{-1/2}u, \ \mathfrak{v} = \beta^{-1/2}v, \ \theta = \pi/2 - \phi, \ r = r, \tag{21}$$

respectively. With this notation we state the following theorem

THEOREM 6.   *The diffeomorphism F_2 transforms the system (6) with potential $U(\theta) = \sin^3 \theta + \beta \cos^3 \theta$ and energy h into the system with potential $V(\theta) = \sin^3 \theta + \beta^{-1} \cos^3 \theta$ and energy $\beta^{-1}h$.*

Proof.   Recall that the McGehee equations are

$$\rho' = \rho \, v, \quad v' = u^2 - \tfrac{3}{2} \, v^2 + 3 \left(\sin^3 \theta + \beta \cos^3 \theta \right),$$
$$\theta' = u, \ u' = -\tfrac{5}{2} u \, v + 3 \sin \theta \cos \theta \left(\sin \theta - \beta \cos \theta \right),$$

with the energy relation

$$\frac{1}{2} \left(u^2 + v^2 \right) - \sin^3 \theta - \beta \cos^3 \theta = \rho^3 h.$$

Through the change of variables given by the diffeomorphism F_2 and making $\theta = \frac{\pi}{2} - \phi$, we obtain the equations

$$\rho' = -\rho \beta^{1/2} \mathfrak{v}, \quad \mathfrak{v}' = \beta^{1/2} \left(\mathfrak{u}^2 - \tfrac{3}{2} \mathfrak{v}^2 \right) + 3\beta^{1/2} \left(\sin^3 \phi + \beta^{-1} \cos^3 \phi \right)$$
$$\phi' = -\beta^{1/2} \mathfrak{u}, \quad \mathfrak{u}' = \tfrac{5\beta^{1/2}}{2} \mathfrak{u}\mathfrak{v} + 3\beta^{1/2} \sin \phi \cos \phi \left(\beta^{-1} \cos \phi - \sin \phi \right),$$

and the energy relation

$$\frac{1}{2} \left(\mathfrak{u}^2 + \mathfrak{v}^2 \right) - \sin^3 \phi - \beta^{-1} \cos^3 \phi = \beta^{-1} \rho^3 h.$$

With a change of time scale to eliminate the factor $\beta^{1/2}$, the transformed equations are

$$\rho' = -\rho \mathfrak{v}, \quad \mathfrak{v}' = \left(\mathfrak{u}^2 - \tfrac{3}{2}\mathfrak{v}^2 \right) + 3 \left(\sin^3 \phi + \beta^{-1} \cos^3 \phi \right)$$
$$\phi' = -\mathfrak{u}, \quad \mathfrak{u}' = \tfrac{5}{2}\mathfrak{u}\mathfrak{v} + 3 \sin \phi \cos \phi \left(\beta^{-1} \cos \phi - \sin \phi \right).$$

These equations coincide with the original ones, except that β is replaced by β^{-1}. In particular $U(\theta) = 0$ if and only if $\tan^3 \theta = -\beta$ if and only if $\tan^3 \left(\frac{\pi}{2} - \theta \right) = -\beta^{-1}$ or $\tan^3 \phi = -\beta^{-1}$.   ∎

Notice that since we are working with McGehee coordinates, this theorem implies an equivalence between the flows on the infinity manifolds. Diffeomorphism F_1 is the same as F_2 but in the original coordinates. It is canonical, but however it does not cover the infinity manifold, as we know.

The topology of N_∞ is a "peanut shaped figure" in this case, except at $\beta = 0$, where we get type $\{2, 4\}$ and N_∞ is a sphere with two cusp points. In the generic case, we denote by A_+, B_+ the attractor points on N_∞ corresponding to the maxima of U, and by $S_\pm$ the saddle points. The θ-coordinate of A_+, $S_\pm$ and B_+ are, in increasing order 0, θ_*, $\pi/2$, respectively.

The positive part of the corresponding function $U(\theta)$ modulo 2π is defined on an interval $(I_0(\beta), I_1(\beta))$, of length π, with $I_0(\beta) \in [-\pi/2, 0]$ and $I_1(\beta) \in [\pi/2, \pi]$. By the translation $\theta \longmapsto \theta + I_0(\beta)$, the point $(I_0(\beta), 0, 0)$ becomes the origin $O = (0, 0, 0)$ and the point $(I_1(\beta), 0, 0)$ becomes $(\pi, 0, 0)$ and the new potential is $U_\beta(\theta) = U(\theta + I_0(\beta))$.

Because of the symmetry (8) of the solutions of system (6), which can be easily verified, it is enough to study the behavior of the two solutions having as initial conditions the points $(0, 0, 0)$ and $(\pi, 0, 0)$. Let us denote these solutions by γ and δ, respectively. These solutions allow us to find the separatrices of the flow on N_∞, and hence they determine it completely. Moreover, these solutions are symmetrical with respect to the plane $v = 0$, and it is enough to study the part where $v \geq 0$. The following result refines Theorem 3.5 in [5].

THEOREM 7. *There exist values $0 < \beta_1 \leq \beta_2 < \beta_2^{-1} \leq \beta_1^{-1}$ of β, such that*

(a)For each $\beta \in (0, \beta_1)$, the $\omega-$limit of γ is B_+

(b)If $\beta > \beta_2$, then the $\omega-$limit of γ is A_+, Similarly,

(c)If $\beta \in \left(0, \beta_2^{-1}\right)$, then the $\omega-$limit of δ is B_+

(d)If $\beta > \beta_1^{-1}$, then the $\omega-$limit of δ is A_+

(e)For $\beta = \beta_1$, the solution γ connects the two saddle points S_- and S_+. In the same way, for $\beta = \beta_1^{-1}$, the solution δ connects the same saddle points on the other side of N_∞.

Proof. Eliminating the time in equations of motion (6) with $\rho = 0$ and $d = 3$ and using the energy relation (4), we get the equation

$$\frac{dv}{d\theta} = \frac{5}{2}\sqrt{2U(\theta) - v^2}. \qquad (22)$$

We compare the solutions $v(\theta)$ of this equation with the solutions of a similar equation where $2U(\theta)$ is replaced by a constant $2K$, i.e.

$$\frac{dv}{d\theta} = \frac{5}{2}\sqrt{2K - v^2}. \qquad (23)$$

By direct integration, and assuming the initial condition $v(\theta_0) = 0$, we obtain the solution

$$\bar{v}(\theta) = \sqrt{2K} \sin \frac{5}{2}(\theta - \theta_0), \tag{24}$$

provided that $\frac{5}{2}(\theta - \theta_0) \leq \pi/2$, i.e. $\theta - \theta_0 \leq \pi/5$.

We begin by proving (a). Let us take $\theta_0 = I_0$ and $K = \beta$ and consider the solution (24). In the interval $[I_0, \theta_*]$ the inequality $0 \leq 2U(\theta) - v^2 \leq 2\beta - v^2$ is satisfied; hence in particular

$$v(\theta_*) \leq \bar{v}(\theta_*) = \sqrt{2\beta} \sin \frac{5}{2}(\theta_* - I_0).$$

On the other hand $I_0 = -\arctan \beta^{1/3}$ and $\theta_* = \arctan \beta$ converge to zero as β tends to zero. Then if β is small enough, we have

$$\bar{v}(\theta_*) \leq \frac{\sqrt{2\beta}}{2} < \sqrt{2U(\theta_*)}. \tag{25}$$

So, for this β, we have that

$$v(\theta_*) < \sqrt{2U(\theta_*)}. \tag{26}$$

The second inequality of (25) is true at least for $\beta < 1$, since $U(\theta_*) = \beta(1 + \beta^2)^{1/2}$. To prove the existence of β_1, we just take the supremum of the values of β satisfying (26). Then one verifies that for this value γ has a saddle-saddle connection.

We now prove (b). Assume that $U(\theta, \beta)$ has the following property: There exists an interval $[\theta_0, \theta_1] \subset [I_0, \theta_*]$ such that $\theta_1 - \theta_0 \geq \pi/5$ and $\sqrt{2U(\theta_0)} = \sqrt{2U(\theta_1)} \geq \sqrt{2U(\theta_*)}$. Because of (24), the solution of (23) with $K = U(\theta_0)$ and the initial condition $v(\theta_0) = 0$, attains the value $\sqrt{2U(\theta_0)}$ before $\theta = \theta_1$. Since the right hand side of (23) is greater or equal that the one of (22) in the interval $[\theta_0, \theta_1]$, the solution γ corresponding to $U(\theta, \beta)$ will attain a value greater than $\sqrt{2U(\theta_*)}$ in the same interval. Indeed, such an interval exists for $\beta = 1$, since $\theta_* = \frac{\pi}{4} > \frac{\pi}{5}$.

We claim that if this property is valid for some value $\beta = \beta_2$, the same is true for each $\beta > \beta_2$. Indeed, $\theta_* = \arctan \beta$ is an increasing function of β. Let $\bar{\theta}(\beta)$ be the unique negative solution of the equation

$$U(\bar{\theta}(\beta), \beta) = \frac{\beta}{(1 + \beta_2)^{1/2}} = U(\theta_*, \beta). \tag{27}$$

We will prove that $\bar{\theta}(\beta)$ is a decreasing function of β. From the Implicit Function Theorem we get

$$3 \sin \bar{\theta} \cos \bar{\theta} \left(\sin \bar{\theta} - \beta \cos \bar{\theta} \right) \frac{d\bar{\theta}}{d\beta} + \cos^3 \bar{\theta} = \frac{1}{(1 + \beta^2)^{3/2}}.$$

Solving for the derivative, we have

$$\frac{d\bar{\theta}}{d\beta} = \frac{\beta \left(1 + \beta^2 \right)^{-3/2} - \cos^3 \bar{\theta}}{3 \sin \bar{\theta} \cos \bar{\theta} \left(\sin \bar{\theta} - \beta \cos \bar{\theta} \right)}.$$

From (27), we solve for $-\cos^3 \bar{\theta}$, getting the equation

$$\frac{d\bar{\theta}}{d\beta} = \frac{-\beta^2 \left(1 + \beta^2 \right)^{-3/2} + \beta^{-1} \sin^3 \bar{\theta}}{3 \sin \bar{\theta} \cos \bar{\theta} \left(\sin \bar{\theta} - \beta \cos \bar{\theta} \right)}.$$

Since $-\frac{\pi}{2} < \bar{\theta} < 0$, we see that $\frac{d\bar{\theta}}{d\beta} < 0$, as asserted.

Now, β_2 is the infimum of the values of β for which the ω−limit of γ is A_+. The rest of the proof follows from the symmetry $\beta \to \beta^{-1}$. ∎

Numerical evidence shows that indeed $\beta_1 = \beta_2$ in the above theorem, but we have not been able to prove it. We have also that $\beta_1 \approx 0.2$.

4. GLOBAL FLOW FOR $H < 0$

In this section we study the global flow on the extended energy levels $E_h \cup N_\infty$ for $h < 0$. In this case these levels are compact manifolds with boundary. Their flow is gradient-like everywhere, and it is completely described by the blow up coordinates. The only case where the global flow needs to be explicitly described is for the peanut shaped manifolds. We give here a thorough description for the case $\alpha = 0$, which is esentially qualitative and depends only on the behavior of some separatrix curves. Recall from Theorem 4 that any pair of middle equilibrium points $S_\pm$ where $U'' > 0$ have 2-dimensional invariant submanifolds propagating and intersecting transversally along the corresponding homothetic orbit. In fact, when the flow is restricted to the boundary, $S_\pm$ are saddle points. Because of the gradient-like structure, the global flow on the extended energy level depends on the global behavior of the separatrices of the saddles. More precisely, it depends on the stable separatrices of S_+ and the unstable separatrices of S_-. This permits us to describe how the whole invariant 2-dimensional submanifolds propagate globally with the flow on $E_h \cup N_\infty$. This is because those submanifolds contain all the separatrices.

Generically and by symmetry, it is enough to consider two cases: $\beta_2 < \beta < \beta_2^{-1}$ and $\beta < \beta_1$.

1) Case $\beta_2 < \beta < \beta_2^{-1}$. This is the simplest one. Consider first the flow on N_∞ and the separatrices of $S_\pm$. Those on the right of the Figure 2, that is $(\theta > \theta_*)$ have B_+ as $\omega-$limit or B_- as $\alpha-$limit. Symmetrically, separatrices on the left of the figure have A_+ as $\omega-$limit or A_- as $\alpha-$limit.
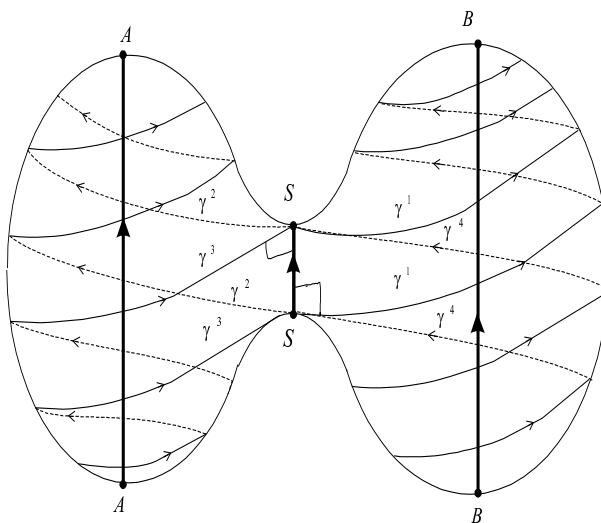
FIG. 2. Separatrices $\gamma_\pm^j$ for the flow on N_∞ for the case $\beta_2 < \beta < \beta_2^{-1}$, together with the homothetic solutions in the energy surface. Superindices 1,2 correspond to the unstable ones, while 3,4 are the stable ones. Index $+$ corresponds to saddle point S_+ and index $-$ to saddle point S_-. Small flags are invariant surfaces in the whole manifold $E_h \cup N_\infty$.

Looking at the flow on the manifold with boundary $E_h \cup N_\infty$, we have the 2-dimensional stable submanifold of S_+ and also the 2-dimensional unstable submanifold of S_- intersecting transversally along the homothetic orbit. Because of the saddle structure of S_+ and S_- on N_∞, these invariant submanifolds will match with separatrices at the opposite point, as shown in Figure 3.

Hence, this intersection acts as a double hinge, which separates completely the flow into 4 disjoint regions in E_h. We describe the flow in these 4 open regions and the boundaries in between, refering to separatrix orbits $\gamma_\pm^j$ as in Figure 2:

i) For any initial condition between submanifolds bounded by orbits $\gamma_\pm^1$ and $\gamma_\pm^3$, the corresponding solution moves close to N_∞, having B_+ as $\omega-$limit and A_- as $\alpha-$limit.
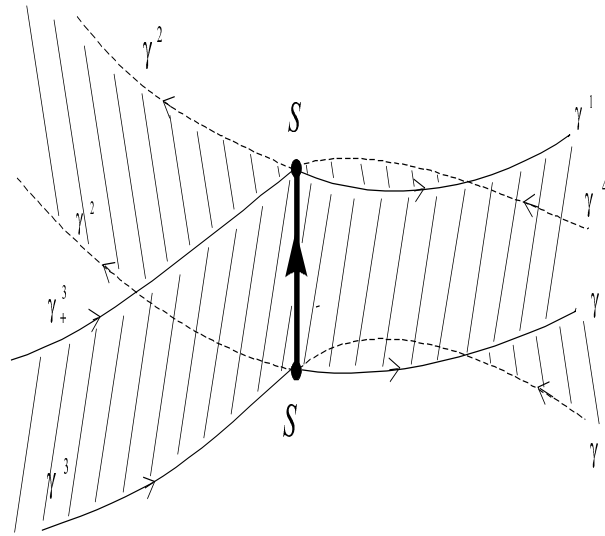
FIG. 3. A close up of Figure 2, where we see how infinite strips are propagated from the invariant surfaces of the $S_\pm$, dividing E_h into four regions.

ii) If the initial condition is located between submanifolds bounded by orbits $\gamma^2_\pm$ and $\gamma^4_\pm$, the orbit moves close to N_∞ and has A_+ as $\omega-$limit and B_- as $\alpha-$ limit.

iii) For any initial condition between submanifolds bounded by $\gamma^1_\pm$ and $\gamma^4_\pm$, the orbit has B_+ as $\omega-$limit and B_- as $\alpha-$limit, remaining only on the right side of the figure.

iv)For any initial condition between submanifolds bounded by $\gamma^2_\pm$ and $\gamma^3_\pm$, the corresponding orbit remains only on the left side of the figure and has A_+ as $\omega-$limit and A_- as $\alpha-$limit.

v) If the initial point happens to be in one of the invariant surfaces, then the orbit remains always on either the left or the right side of the figure with respect to the homothetic orbit. It has either S_- as $\alpha-$limit or S_+ as $\omega-$limit.

2) Case $\beta < \beta_1$. As in the previous case, separatrices on the right have B_+ as $\omega-$limit and B_- as $\alpha-$limit. But the situation is not symmetrical on the left side. The difference is that the unstable separatrix γ^2_- having S_- as $\alpha-$limit has B_+ as $\omega-$limit instead of A_+, while separatrix γ^3_+ having S_+ as $\omega-$limit goes around and has B_- as $\alpha-$limit instead of A_-. Again the homothetic orbit with the two invariant submanifolds generate a double hinge, but the separation of E_h into regions becomes more complicated as we describe below. In comparison with the case 1), as β varies one has

passed for $\beta = \beta_1$ through a saddle connection bifurcation where $\gamma_-^2 = \gamma_+^3$ holds.

The problem is with the propagation by the flow of a portion of the invariant submanifolds bounded by $\gamma_\pm^2$ and $\gamma_\pm^3$. Because of symmetry (8) it is enough to describe one of two, say the first one, as depicted in Figure 4.
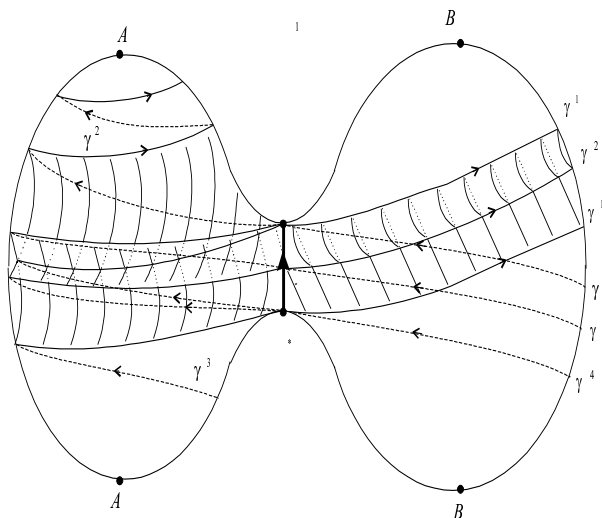
FIG. 4. The small channel is bounded by strips $\gamma_+^1\gamma_-^2$ and $\gamma_+^1\gamma_-^1$ on the right side. See explanation in the text.

Since γ_-^2 has B_+ as $\omega-$limit, it crosses to the right side after one turn around the homothetic orbit, while γ_+^2 stays always on the left. This forces a splitting of the corresponding invariant surface into two portions: one of them stays on the left, while the other one passes to the right. The first one is generated between two consecutive turns of γ_+^2. The other one runs between γ_+^1 and the part of γ_-^2 on the right side, but closer to N_∞ than the invariant manifold bounded by $\gamma_\pm^1$ (unstable manifold of S_-). We call this second portion a small channel, because of the way it runs closer to N_∞. Transversal sections $\theta < \theta_*$, $\theta = \theta_*$ (passing through S_+ and S_-) and $\theta > \theta_*$ of Figure 4 are depicted in Figure 5.

In these sections, the traces of N_∞ are ovals, invariant submanifolds are curves inside the ovals, intersecting the ovals at points representing traces of the separatrices. In the figure $\theta < \theta_*$, the invariant submanifolds $W_{S_-}^u$ has 2 intersections: the curve $\gamma_+^2\gamma_-^2$ and also the curve $\widetilde{\gamma_+^2}\widetilde{\gamma_-^2}$. The last one corresponds to later times along the flow, so that the invariant
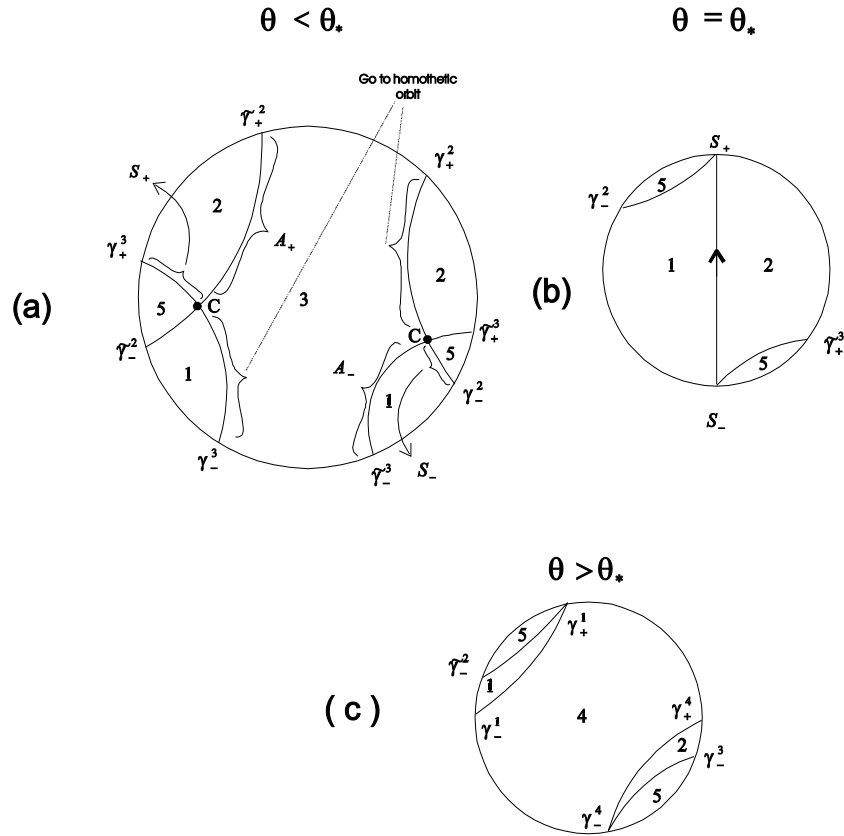
FIG. 5. Transversal slices of N_∞ and the invariant strips in Figure 4. The small channels appear as regions 1 and 2 when we pass to $\theta > \theta_*$.

submanifold went around the homothetic orbit joining A_- with A_+ and came back close to our main homothetic orbit at $\theta = \theta_*$. Similarly, the invariant submanifold $W^s_{S_+}$ has as intersections the curves $\gamma^3_+\gamma^3_-$ and $\widetilde{\gamma^3_+}\widetilde{\gamma^3_-}$ with the same interpretation as above, only that the last one corresponds to earlier times along the flow. From those curves, we see that in said section, $W^u_{S_-}$ and $W^s_{S_+}$ intersect in the heteroclinic solution C, whose trace point is shown on both sides where the trace curves intersect. This heteroclinic connection is in E_h, but very close to N_∞, as Figure 4 depicts in $E_h \cup N_\infty$.

The ovals and the curves inside them divide into 4 distinct regions numbered 1, 2, 3, 5. The couples of regions with the same number are connected in E_h in between the invariant submanifolds.

As we pass to section $\theta = \theta_*$, the vertical line corresponds to the homothetic orbit. Regions 1 and 2 have become big since they correspond to 2 sides of the double hinge, while region 3 disappeared since it was on the side $\theta < \theta_*$ of the hinge. The smaller region 5 (2 components) corresponds to the beginning of the small channels. The upper component is bounded by a portion of $W^u_{S_-}$, while the lower one is bounded by a portion of $W^s_{S_+}$.

In section $\theta > \theta_*$ we have a big new region numbered 4, corresponding to the fourth side of the double hinge for $\theta > \theta_*$. Regions 1, 2 and 5 have now shrunk. The last one is the continuation of the small channel.

This way we can describe precisely the $\alpha-$ and $\omega-$ limits of orbits on the 5 open regions as follows

Region	$\alpha-$limit	$\omega-$limit
1	A_-	B_+
2	B_-	A_+
3	A_-	A_+
4	B_-	B_+
5	B_-	B_+.

The $\alpha-$ and $\omega-$limit for the heteroclinic connection C are S_- and S_+, respectively.

Orbits in region 5 necessarily pass to the portion $\theta < \theta_*$ in some bounded time interval. Only the first 4 regions were present in case 1) considered earlier.

Finally, the only portions of invariant submanifolds changing from one side to the other of Figure 5 for the extended energy level are

(a) The boundary between regions 1 and 5, contained in $W^u_{S_-}$. Its $\omega-$limit is B_+, exactly like γ^2_-

(b) The boundary between regions 2 and 5, contained in $W^s_{S_+}$. Its $\omega-$limit is B_-, exactly like γ^3_+.

This global behavior has been verified by computer simulations.

5. SOME NUMERICAL SIMULATIONS FOR NEGATIVE AND POSITIVE ENERGY

In this section, we describe some numerical simulations to visualize some aspects of the global dynamics described in the previous section. Also, a

sketch of the flow for positive energy is given to get an idea of this case, which is more complicated than the corresponding to negative energy. This ilustrates some of the difficulties for the case of positive energy.

In Figure 6, the projection on the plane $v - \theta$, of the manifold N_∞ and several trajectories of the flow for $\beta = 1$ are shown; this value of β belongs to the interval $\left(\beta_2, \beta_2^{-1}\right)$. We use heavy lines to draw the invariant manifolds of S_+ and S_-. The discontinuous line indicates that the curve is on the back part of N_∞, that is $(u < 0)$.
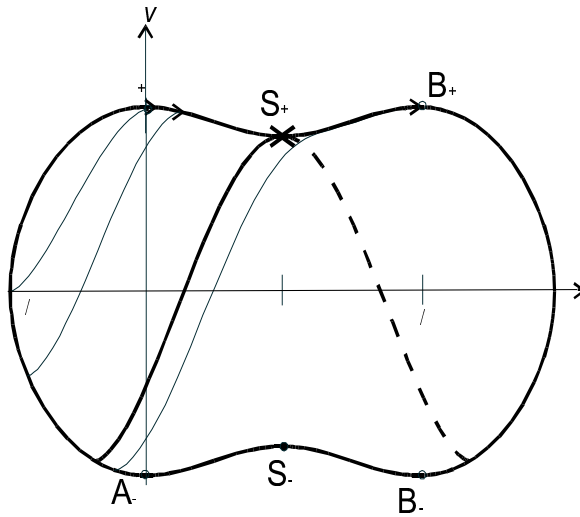
FIG. 6. Flow on N_∞ for $\beta_2 < \beta < \beta_2^1$.

We assume that from now on $\theta > \theta_*$. We know from the previous section that trajectories which start between N_∞ and $W_{S_+}^s$ have A_+ as $\omega-$limit. When the trajectory starts between $W_{S_+}^s$ and $W_{S_-}^u$, its $\omega-$limit is B_+; moreover, if the starting point is close enough to $W_{S_+}^s$, its θ coordinate is a decreasing function of τ, in an interval of the form $[0, \widetilde{\tau}]$ and is bounded below by θ_*. If the orbit starts between $W_{S_-}^u$ and N_∞, then its $\omega-$limit is B_+. In this case the θ coordinate is an increasing function for small and positive τ. These features can be observed by performing numerical computations of the orbits, in the following way.

We fix $\overline{\theta}$ and $\overline{v}$ such that $\overline{\theta} > \theta_*$ and $-\sqrt{2U\left(\overline{\theta}\right)} < \overline{v} < \sqrt{2U\left(\overline{\theta}\right)}$. The half-ray $\left\{v = \overline{v}, \theta = \overline{\theta}\right\}$ intersects N_∞ at the points $P_I\left(\overline{\theta}, \overline{v}, -\overline{u}\right)$, $P_F\left(\overline{\theta}, \overline{v}, \overline{u}\right)$ for some $\overline{u} > 0$. For any positive integer number we define in the segment $[P_I, P_F]$, the partition $\{P_i\}_{i=0}^n$, with $P_i = \left(\overline{\theta}, \overline{v}, -\overline{u} + \frac{2i\overline{u}}{n}\right)$. We take P_i

as initial condition. When i increases from 0 to n, there appear regions of different behaviour of the flow. Thus, there are indices $i_1 < i_2$ such that the manifold $W^s_{\hat{S}_+}$ is between P_{i_1} and P_{i_1+1}, and the manifold $W^u_{\hat{S}_-}$ is between P_{i_2} and P_{i_2+1}. As n increases we get better approximations. In Figure 7 we have $\overline{\theta} = \frac{3\pi}{8}$, $\overline{v} = 0$, $\overline{u} = -\sqrt{2U(\overline{\theta})} \approx 1.29971$. For $n = 100$, we get $i_1 = 15$ and $i_2 = 84$.
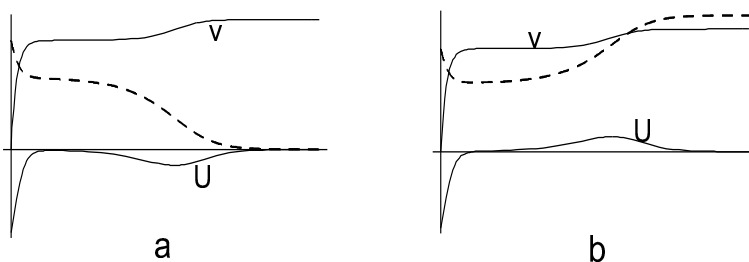
FIG. 7. Components of trajectories starting from points P_{15} (part (a)) and P_{84} (part(b)) as functions of τ, for case $\beta_2 < \beta < \beta_2^{-1}$.

In the part (a) of Figure 7, the trajectory has the point $A_+ = \left(0, \sqrt{2}, 0\right)$ as $\omega-$limit. In part (b) of Figure 7 the trajectory goes to $B_+ = \left(\pi/2, \sqrt{2}, 0\right)$. To calculate i_2 we solve numerically the system with τ running to $-\infty$. So, we see that the $\alpha-$limit of the trajectory corresponding to P_{84} is B_- and the $\alpha-$limit of the orbit corresponding to P_{85} is A_-.

For $\beta < \beta_1$, the situation is different due to the presence of the "small channels" in the invariant manifolds (see Section IV). The trajectories in the region $\theta > \theta_*$, whose initial point is inside of the small channels have as $\omega-$limit the point A_+. If we consider a partition as in the above case, and the corresponding segment crosses through the small channel, we get indices i_1, i_2 such that, for all $i \leq i_1$, the $\omega-$limit of the orbits is B_+. When $i_1 < i < i_2$, the $\omega-$limit is A_+ and for $i \geq i_2$, the $\omega-$limit is B_+.

To locate numerically the small channel for $\beta = .15$ one considers now the segment $[P_I, P_F]$ defined by $\overline{\theta} = 0.149$, $\overline{v} = -.5447$, $\overline{u} = 72.1 \times 10^{-6}$. With $n = 1000$, the value of i_1 is 291 (see (A) of Figure 8)

Notice that θ takes negative values, which means that the orbit goes around the homothetic orbit from A_- to A_+, before it reaches the point $B_+ = \left(\pi/2, \sqrt{2}, 0\right)$. The trajectory in (B) of Figure 8 has a $\omega-$limit the point $A_+ = \left(0, \sqrt{.3}, 0\right)$. When $i_2 = 293$, the corresponding orbit has again as $\omega-$limit the point B_+.

When the energy h is positive, the flow given by (6) is not any more gradient-like with respect to any of the variables ρ, θ, v, u, except on N_∞ Due to this fact the flow is more complicated than the corresponding
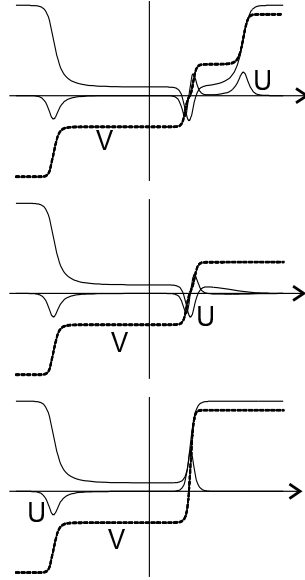
FIG. 8. Components of trajectories starting from points P_i, for $i = 291, 292, 293$. For points P_{291} and P_{293} the $\omega - limit$ is B_+, while the $\omega - limit$ for P_{292} is A_+. This is due to the existence of the small channel.

to negative energy and of course it is more difficult to give a complete description of the global behaviour of the flow.

In what follows, we describe some numerical simulations to get an idea of the main features of this flow, when N_∞ consists of three connected components, each one topologically equivalent to the sphere S^2. Indeed, we consider $U(\theta) = \sin^3 \theta - 3 \cos \theta \sin^2 \theta + \cos^3 \theta$. In this case the flow has 6 equilibrium points

$$Q_1 = \left(0, \sqrt{2}, 0\right) \; ; \; Q_1' = \left(0, -\sqrt{2}, 0\right),$$
$$Q_2 = \left(\theta_{2_*}, \sqrt{2U(\theta_{2_*})}, 0\right) \; ; \; Q_2' = \left(\theta_{2_*}, -\sqrt{2U(\theta_{2_*})}, 0\right),$$
$$Q_3 = \left(\theta_{3_*}, \sqrt{2U(\theta_{3_*})}, 0\right) \; ; \; Q_3' = \left(\theta_{3_*}, -\sqrt{2U(\theta_{3_*})}, 0\right),$$

here $0, \theta_{2_*}, \theta_{3_*}$ are the first 3 non negative values of θ, where U has a local maximum. The approximate values are $\theta_{2_*} = 1.9804$, $v_2^* = \sqrt{2U(\theta_{2_*})} = 1.8514$, $\theta_{3_*} = 4.0577$, $v_3^* = \sqrt{2U(\theta_{3_*})} = 0.9214$.

On the segment $\{-0.488 \leq \theta \leq 4.378, v = 2.5, u = 0\}$ we take the partition $\{P_i\}_{i=0}^{80}$, with $P_i = (-0.488 + i\Delta\theta, 2.5, 0)$ and $\Delta\theta = \frac{4.378+0.488}{80}$. The system 6 was numerically integrated with Mathematica taking P_i as initial condition, for $i = 0, \cdots, 80$. We see that the orbits whose $\alpha-$limit is Q_1' are the ones corresponding to the points in the intervals $I_1 = [P_{42}, P_{59}]$, $I_2 = [P_{62}, P_{73}]$. For convenience we identify below the initial condition with its orbit. The trajectories of I_1 have as $\omega-$ limit the point Q_2 and the $\omega-$limit of I_2 is Q_3. Notice that the trajectory P_{60} converges to Q_1, whereas P_{61} converges to Q_3 and both trajectories tend to ∞ when τ tends to $-\infty$. Also their corresponding $\theta-$coordinate grow up without limit. All these facts imply the existence of trajectories which come spiralling from the origin . Moreover, between P_{60} and P_{61} there is an invariant separatrix of the flow. (See Figure 9)

FIG. 9. Trajectories with initial conditions in a fixed segment $u = 0, v = 2.5$ having as $\alpha - limit \; Q_1'$. The energy is positive and N_∞ has three components.

The trajectories of the intervals $I_3 = [P_0, P_6]$ and $I_4 = [P_{76}, P_{80}]$ have as $\alpha-$limit the point Q_2'. The $\omega-$limit of I_3 is Q_1 and the $\omega-$limit of I_4 is Q_3. (See Figure 10).

The point Q_3' is the $\alpha-$limit of the orbits in $I_5 = [P_{11}, P_{22}]$ and $I_6 = [P_{24}, P_{39}]$. The $\omega-$limit of I_5 is Q_1 and Q_2 is the $\omega-$limit of I_6. The orbit P_{23} converges to Q_1 and comes from ∞. So, we have a situation similar to that between P_{60} and P_{61}, described above. (See Figure 11).

FIG. 10. Trajectories with initial conditions in a fixed segment $u = 0, v = 2.5$ having as $\alpha - limit\ Q'_2$. The energy is positive and N_∞ has three components.
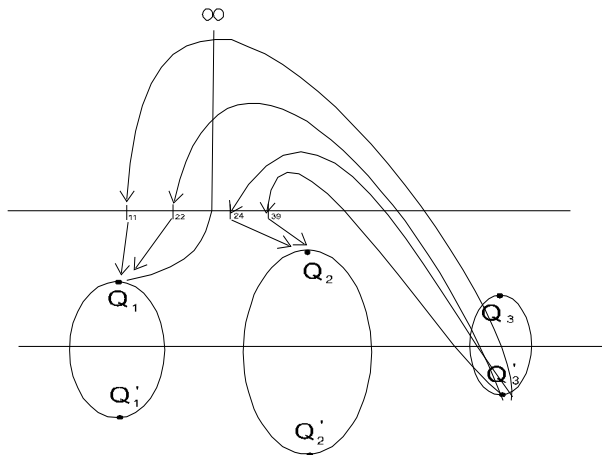
FIG. 11. Trajectories with initial conditions in a fixed segment $u = 0, v = 2.5$ having as $\alpha - limit\ Q'_3$. The energy is positive and N_∞ has three components.

Finally, the intervals $[P_7, P_{10}]$, $[P_{40}, P_{41}]$, $[P_{73}, P_{75}]$ are close to the homothetic orbits, so their trajectories have a behaviour similar to these homothetic orbits. (See Figure 12).

We remark an apparent duality between the dynamics for $h < 0$ and for $h > 0$. The most complicated case for $h < 0$ is the one corresponding to the peanut shaped N_∞, while the most complicated case for $h > 0$ seems to
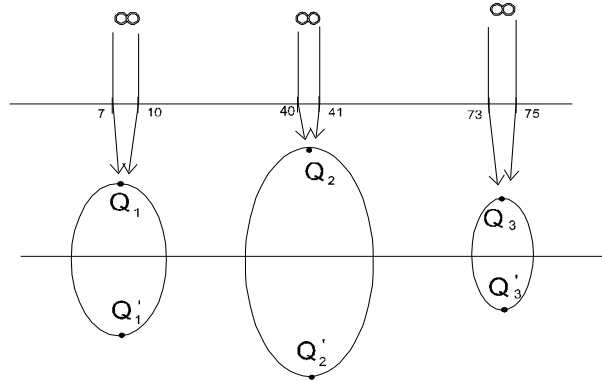
FIG. 12. Trajectories with initial conditions in a fixed segment $u = 0, v = 2.5$ which are close to the homothetic orbits for negative *tau*.

be when N_∞ is a disjoint union of three spheres, which we have considered above.

6. ACKNOWLEDGMENTS

REFERENCES

1. J. DELGADO-FERNÁNDEZ AND E. PÉREZ-CHAVELA, *The rhomboidal four body problem. Global solution on the total collision Manifold* in T. Ratiu, (ed.), The Geometry of Hamiltonian Systems, Springer-Verlag (1991), 97-110.

2. F.N. DIACU, *On the validity of Mücket-Treder gravitational law*, in E. Lacomba and J. Llibre, (eds.), New trends in Hamiltonian Systems and Celestial Mechanics, World Scientific Publ., Singapore (1995), 127-139.

3. F.N. DIACU, *Collision/ejection dynamics for particle systems with quasihomogeneous potentials*, (To appear)

4. M. FALCONI, *Estudio asintótico de escapes en sistemas Hamiltonianos Polinomiales.* P.H. Dissertation, UNAM (1996).

5. M. FALCONI AND E.A. LACOMBA, *Asymptotic behavior of escape solutions of mechanical systems with homogeneous potentials*, Cont. Math. **198**, (1996), 181-195.

6. B. GRAMMATICOS AND B. DORIZZI, *Integrability of Hamiltonian with third and fourth degree polynomial potentials*, J. Math. Phys. **24** (9), (1983), 2289-2295.

7. E.A. LACOMBA, *Infinity manifold for positive energy in celestial mechanics*, Contemporary Math. **58**, part III, (1987), 193-201.

8. E.A. LACOMBA AND L.A. IBORT, *Origin and infinity manifolds for mechanical systems with homogeneous potentials*, Acta App. Math. **11**, (1988), 259-284.

9. E.A. LACOMBA, J. BRYANT AND L.A. IBORT, *Blow up of mechanical systems with a homogeneous energy*, Publ. Math. **35**, (1991), 333-345.

10. R. MCGEHEE, *Triple collision in the colinear three body problem*, Inventiones Math., **27**, (1974), 191-227.

11. C. SIMO AND E. A. LACOMBA, *Analysis of some degenerate quadruple collisions*, Celestial Mechs.**28**, (1982), 49-62.